Korea-Australia Rheology Journal
Vol. 17, No. 3, September 2005 pp. 125-130

Coalescence behavior of dispersed domains in binary immiscible fluid mixtures having bimodal size distributions under steady shear flow

Yoshiaki Takahashi* and Tsuyoshi Kato
Department of Molecular and Material Sciences, IGSES, Kyushu University, 6-1 Kasugakoen, Kasuga 816-8580 JAPAN

(Received, April 27, 2005)

Abstracts

Coalescence process of binary immiscible fluid mixtures having bimodal size distributions, prepared by mixing two pre-sheared samples at different shear rates, $\dot{\gamma}_{pre1}$ and $\dot{\gamma}_{pre2}$, under shear flow at a final shear rate, $\dot{\gamma}_f$, are examined by transient shear stress measurements and microscopic observations in comparison with the results for simply pre-sheared samples having narrow size distributions (unimodal distribution samples). Component fluids are a silicone oil (PDMS) and a hydrocarbon-formaldehyde resin (Genelite) and their viscosities are 14.1 and 21.0 pa·sec at room temperature (*ca.* 20°C), respectively. The weight ratio of PDMS: Genelite was 7:3. Three cases, ($\dot{\gamma}_{pre1} = 7.2$ sec^{-1}, $\dot{\gamma}_{pre2} = 12.0$ sec^{-1} and $\dot{\gamma}_f = 2.4$ sec^{-1}), ($\dot{\gamma}_{pre1} = 0.8$ sec^{-1}, $\dot{\gamma}_{pre2} = 4.0$ sec^{-1} and $\dot{\gamma}_f = 2.4$ sec^{-1}), and ($\dot{\gamma}_{pre1} = 7.2$ sec^{-1}, $\dot{\gamma}_{pre2} = 12.0$ sec^{-1} and $\dot{\gamma}_f = 7.2$ sec^{-1}) are examined. In the first case, transient shear stress did not show any significant difference but domains larger than the initial state are observed at short times. In the latter cases, there exist undershoot of shear stress, reflecting existence of deformed large domains, which is confirmed by the direct observation. It is concluded that coalescence between large and small domains more frequently occur than coalescence between the domains with similar size in the bimodal distribution samples.

Keywords : immiscible polymer blends, domain size distribution, coalescence process

1. Introduction

Studies on flow-induced structure and the related viscoelastic properties of emulsions and immiscible polymer blends under shear flows have a long history. After the pioneering work of Taylor (1932; 1934), many relationships between viscosity and domain structure have been discussed as summarized by Utracki (1989). In the last two decades, new theories apparently including the characteristic behaviors of elastic parameters have been published, for example, by Doi and Ohta (1991). At the same time, new experimental techniques are developed, which enabled us the direct observation of structural changes under the successive increase or decrease of shear rates. Hence more systematic studies on the relationships between the structural changes and the rheological properties become possible as summarized by Nakatani and Dadmun (1995).

Among them, break-up of relatively large domains after stepwise increase of shear rates from $\dot{\gamma}_i$ to $\dot{\gamma}_f$ (break-up process) and coalescence of relatively small domains after stepwise decrease of shear rates from $\dot{\gamma}_i$ to $\dot{\gamma}_f$ (coalescence process) are mainly examined by the studies of model blend systems, that is, binary mixtures of immiscible fluids having constant viscosities and their ratio not so far from unity by Takahashi *et al.* (1994a; 1994b), by Takahashi and Noda (1995), by Vinckier *et al.* (1996), and Kitade *et al.* (1997). The steady state values of (excess) shear stress σ and (excess) first normal stress difference N_1 are proportional to $\dot{\gamma}$ in the both processes. The shorter diameters of ellipsoidal domains observed at steady states and/or radii of relaxed spherical domains observed after cessation of the steady shear flow show narrow size distributions and their average values are inversely proportional to the shear rate.

In the break-up process, elliptically deformed domains under the initial steady state are extremely elongated, followed by rupture and gradual approach to smaller ellipsoidal domains at the final steady state. An undershoot and an overshoot of transient shear stress and first normal stress difference, $\sigma(t)$ and $N_1(t)$, corresponding to the above structural changes are observed. In the coalescence process, very slow coalescence of the domains and monotonic increase of stresses are observed. The rescaled stresses (i.e., $\sigma(t)$ and $N_1(t)$ divided by their initial steady values, σ_i and N_{1i}, respectively) at constant $\dot{\gamma}_f/\dot{\gamma}_i$ in the both processes compose respective master curves as a function of

*Corresponding author: ytak@mm.kyushu-u.ac.jp

strain $\dot{\gamma}_f t$, where t is the time after the change of shear rate. All these behaviors are qualitatively consistent with the scaling relations predicted by Doi and Ohta (1991), implying that the domain structure and the related rheological properties are determined by the flow field independent of the flow history. It is also known that there exist upper and lower critical shear rates in the break up process. At very high shear rates, domains hardly break up, while at very low shear rates, domain size distribution become broad and the reproducibility of the rheological data become poor as pointed out by Kitade *et al.* (1997).

Recently, hysteresis in the shear rate dependence of domain size was reported at relatively low shear rates by Rusu and Peuvrel-Disdier (1999). Takahashi and Akazawa (2005) discussed such hysteresis behavior of domain size in break-up and coalescence processes based on the applicability of Doi-Ohta theory. Below the critical shear rate, where the theory is not applicable, domain size in the break-up process is not well controlled by the flow resulting in the broad size distribution and poor reproducibility of shear viscosities. However, shear rate dependence of average domain size is practically the same as that observed above the critical shear rate. On the other hand, the domain size observed in the coalescence process has narrow size distribution being well controlled by the flow and the viscosity is reproducible but the shear rate dependence of domain size is lower than that observed above the critical shear rate.

All above studies are performed after a certain pre-shear, implying that the size distributions at initial states are unimodal. In practice, size distributions of immiscible fluids are not always unimodal. For more systematic understanding of flow induced structural change of dispersed domains, we report coalescence behaviors of mixtures of two differently pre-sheared samples in comparison with those of simply pre-sheared samples.

2. Experimental

Two component samples used are a silicone oil (polydimethylsiloxane : PDMS) from Shinetsu Chemical Co. and a hydrocarbon-formaldehyde resin (Genelite) from General Sekiyu K. K. These fluids show Newtonian viscosity behavior in the whole shear rate region examined in this work. Viscosities of PDMS and Genelite are 14.1 and 21.0 pa·sec at room temperature (*ca.* 20°C), respectively. Their blend sample (PDMS:Genelite = 7:3 by weight) was prepared by gently stirring weighed amounts of samples in a vessel with a spatula for a few minutes so that the domain size of typical ones will exceed 100 μ.

Shear stresses of all the samples are measured with Anton Paar MCR300 rheometer. A cone-plate geometry with 50 mm diameter and 3° cone-angle is used. It should be noted that N_1 cannot be detected for all the samples examined in this work since they are too small compared to the reliable measurement range of MCR300. As discussed in a previous work by Takahashi and Akazawa (2005), however, $\sigma(t)$ measurements are enough to discuss the structural change of the samples in this study.

The structural changes of dispersed domains in the samples are observed with a Keyence monitor microscope VH-5910 attached to a Nihon Rheology Kiki RGM-150-NF-S0 rheometer, through the quartz cone (80 mm diameter and 3° cone-angle). During a shear flow, short interruptions are given at desired flow time to record the images of relaxed spherical domains. At each observation, diameters of about hundred domains are analyzed to obtain volume averaged radii R_v and number averaged radii R_n.

The blend samples are pre-sheared at a certain shear rate in cone-plates of MCR300 or RGM-150-NF-S0. At each shear rate, time dependency of $\sigma(t)$ was observed by MCR300 to ensure that the steady state is achieved. After the pre-shear, image of domain structures are recorded. Then the measurements for the unimodal distribution samples after onset of shear flow at $\dot{\gamma}_f$ are started.

A few selected pre-sheared samples with different shear rates, $\dot{\gamma}_{pre1}$ and $\dot{\gamma}_{pre2}$, are carefully taken off from con-plates and poured into a vessel very slowly to prepare their mixtures, i.e., bimodal distribution samples. The mixing ratio was 1:1 by weight. The bimodal distribution samples are carefully set to the rhometers and the measurements are started. All experiments are carried out at room temperature.

3. Results and discussions

Fig. 1 shows examples of histogram of domain size R_i after the pre shear. The top and the middle panels show the data for unimodal distribution samples while the bottom panel shows the data for a bimodal distribution sample. Although, there is no apparent bimodal peak in the bottom panel, this histogram coincide with that calculated from histograms of the two pre-sheared samples. Further, the samples pre-sheared in the hysterisis region defined below, shows broad size distribution. To avoid confusion, we call the mixtures of two pre-sheared samples as bimodal distribution samples and the samples pre-sheared at shear rates in the hysterisis region as broad distribution samples. Further, the samples pre-sheared in the textured region, which is also defined below, are called unimodal distribution samples.

Fig. 2 shows shear rate dependence of number averaged diameter (= $2R_n$) in break up and coalescence processes. As reported by Takahashi and Akazawa (2005), these data can be classified into to groups at a critical shear rate shown by a vertical broken line. Hereafter, we call two regions above and below the critical shear rate as textured region and hysterisis region, respectively. In the textured region, the data

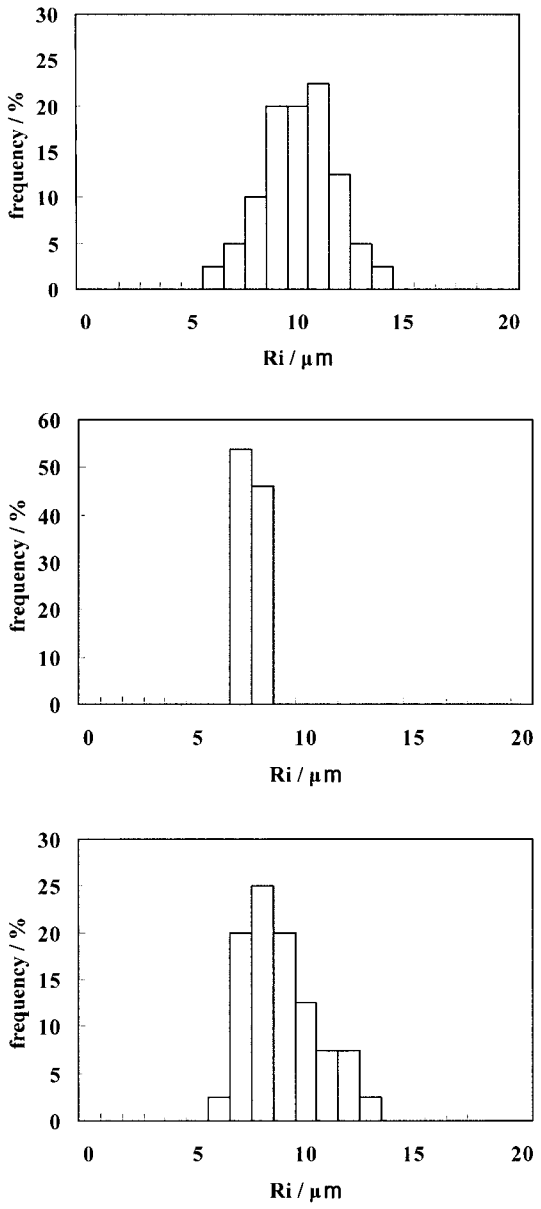

Fig. 1. Examples of histograms of domain size after pre-shear. Shear rates are 7.2 and 12.0 sec^{-1} for the top and middle panels, respectively. The bottom panel shows the histogram obtained for the bimodal distribution sample ($\dot{\gamma}_{pre1}$ = 7.2, $\dot{\gamma}_{pre2}$ = 12.0 sec^{-1}), which is practically the same as that calculated from the data in above two panels.

obtained in the both processes at the same $\dot{\gamma}_f$ become identical and their size distributions are always narrow. In the hysteresis region, domain size distribution of the data for the break-up process become broad but the $\dot{\gamma}$ dependence of R_n is practically the same as that in the textured region, while size distribution for the coalescence process is narrow but shows lower $\dot{\gamma}$ dependence, consistent with the previous study.

Three bimodal distribution samples are examined in this study. The pre- and final shear rates for the first sample are

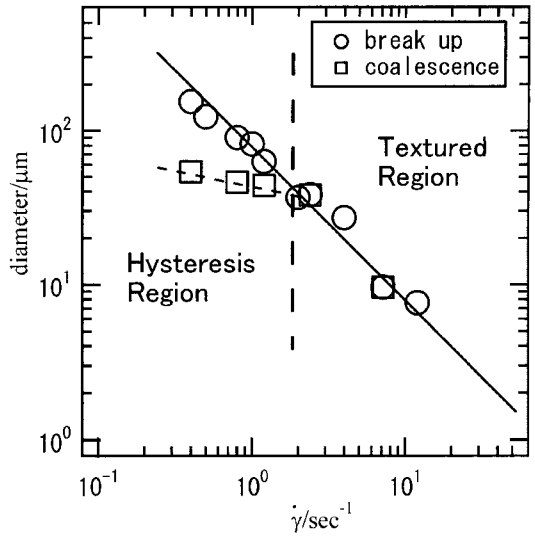

Fig. 2. Shear rate dependence of number average diameters (= $2R_n$) of domains obtained in the break-up and coalescence processes, respectively. Vertical broken line denotes the critical shear rate between hysteresis region and textured region. Solid line denotes the slope −1, while thin broken line is guide for eyes.

$\dot{\gamma}_{pre1}$ = 7.2 sec^{-1}, $\dot{\gamma}_{pre2}$ = 12.0 sec^{-1}, and $\dot{\gamma}_f$ = 2.4 sec^{-1}. In this case, coalescence process will be the dominant process. It is also expected that the final size distribution become narrow since $\dot{\gamma}_f$ is in the textured region. The pre- and final shear rates for the second sample are $\dot{\gamma}_{pre1}$ = 0.8 sec^{-1}, $\dot{\gamma}_{pre2}$ = 4.0 sec^{-1}, and $\dot{\gamma}_f$ = 2.4 sec^{-1}. This sample corresponds to a bimodal sample prepared by mixing broad (pre-sheared in the hysterisis region) and unimodal (pre-sheared in the textured region) distribution samples. In this case, occurrence of both break-up and coalescence processes are expected. The pre- and final shear rates for the third sample are $\dot{\gamma}_{pre1}$ = 7.2 sec^{-1}, $\dot{\gamma}_{pre2}$ = 12.0 sec^{-1}, and $\dot{\gamma}_f$ = 7.2 sec^{-1}. In this case, $\dot{\gamma}_{pre1}$ = $\dot{\gamma}_f$ so that in principle structural change need not occur for the larger domains. In these measurements, the final steady states are not achieved since the characteristic behavior of bimodal distribution samples are observed at relatively short times while the data at long times become almost identical with those of unimodal samples.

Fig. 3 shows transient shear stress $\sigma(t)$ for a unimodal distribution sample ($\dot{\gamma}_{pre}$ = 7.2 sec^{-1}) and a bimodal distribution sample ($\dot{\gamma}_{pre1}$ = 7.2, $\dot{\gamma}_{pre2}$ = 12.0 sec^{-1}) after onset of shear flow. It is clear that $\sigma(t)$ for both samples monotonically increase toward the steady value and their difference are not so significant. Fig. 4 shows examples of histograms for the bimodal distribution sample obtained at different time t. Comparing the histogram at t = 10 min with that before the onset of flow (Fig. 1 bottom), it can be pointed out that the peak position for the smaller domains generated by $\dot{\gamma}_{pre2}$ is not changed while the number of

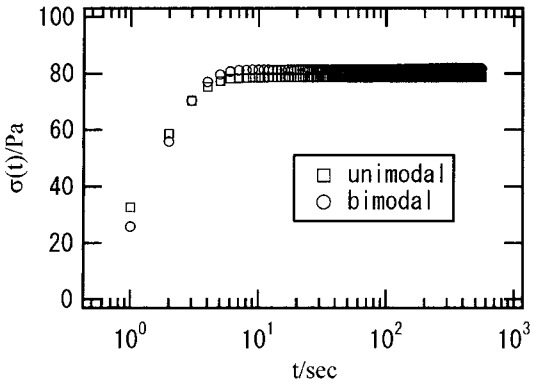

Fig. 3. Transient stress $\sigma(t)$ for a unimodal ($\dot{\gamma}_{pre} = 7.2\ sec^{-1}$) and a bimodal distribution ($\dot{\gamma}_{pre1} = 7.2$, $\dot{\gamma}_{pre2} = 12.0\ sec^{-1}$) samples after the onset of shear flow with $\dot{\gamma}_f = 2.4\ sec^{-1}$.

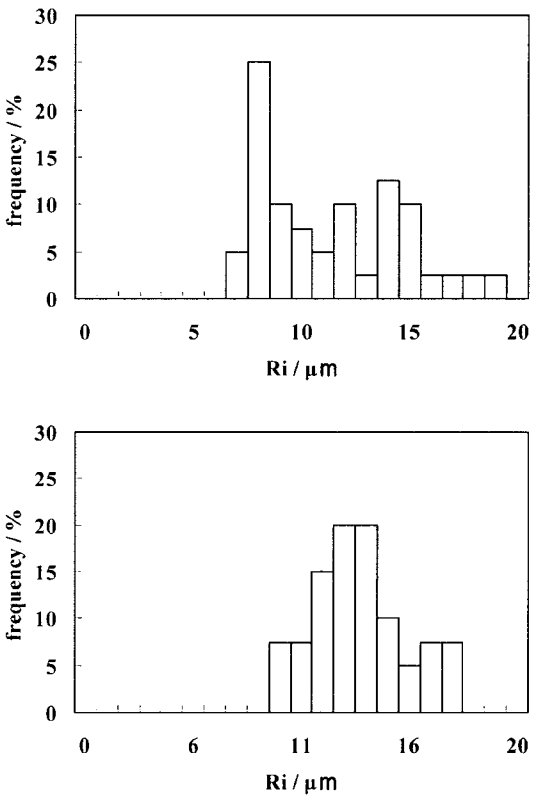

Fig. 4. Examples of histgrams after the onset of shear flow ($\dot{\gamma}_f = 2.4\ sec^{-1}$) for the bimodal distribution ($\dot{\gamma}_{pre1} = 7.2$, $\dot{\gamma}_{pre2} = 12.0\ sec^{-1}$) sample. Observation times are 10 and 120 minutes after the onset of flow for the top and bottom panels, respectively.

domains decrease. On the other hand, the peak position for the larger domains generated by $\dot{\gamma}_{pre1}$ move toward larger size while the number of domains do not change so much, resulting in very broad distribution with two apparent peaks. At $t = 120$ min, some parts of the large domains seems to be broken-up while smaller domains coalesced, resulting in a single peaked histgram.

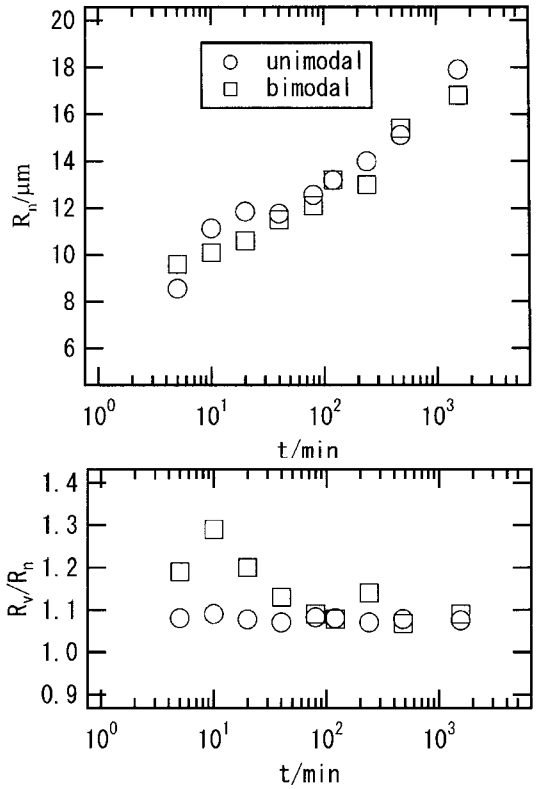

Fig. 5. Time dependencies of R_n and R_v/R_n for the same samples as in Fig. 3.

Fig. 5 compares the flow time dependencies of R_n and R_n/R_v for the same samples as in Fig. 3. It is clear that the time dependencies of R_n data are almost the same but the size distributions are much broader for the bimodal distribution sample at the initial stage of coalescence, while the size distributions of the unimodal distribution sample maintain almost constant. At the later stage, both data become almost identical. Thus, it is concluded that coalescence between large and small domains more frequently occur in the bimodal distribution samples at the initial stage of coalescence. Similar result was obtained by Takahashi and Kato (2005), though the final size distribution was much broader. In this study, $\dot{\gamma}_f$ is in the textured region while $\dot{\gamma}_f$ in previous study is in the hysterisis region, in which broken domains have broad distributions. Therefore, the broader size distribution in the previous work can be attributed to the break-up of large domains generated by the coalescence of large and small domains at the initial stage.

Fig. 6 shows $\sigma(t)$ for the second bimodal sample ($\dot{\gamma}_{pre1} = 0.8$, $\dot{\gamma}_{pre2} = 4.0$, and $\dot{\gamma}_f = 2.4\ sec^{-1}$). There exist a very shallow minimum in the $\sigma(t)$, denoting the existence of elongated domains. Actually, it was confirmed by video microscopic observation under the flow that there exist largely elongated domains. The typical aspect ratios of the domains are around 2, while some thread-like domains extended to the outside of view screen. As reported by

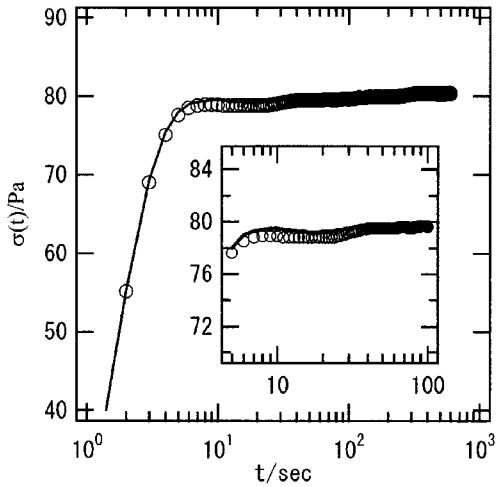

Fig. 6. Transient stress $\sigma(t)$ for a bimodal distribution sample ($\dot{\gamma}_{pre1} = 0.8$, $\dot{\gamma}_{pre2} = 4.0$, and $\dot{\gamma}_f = 2.4\ \mathrm{sec}^{-1}$) and a broad distribution sample ($\dot{\gamma}_{pre} = 0.8$ and $\dot{\gamma}_f = 2.4\ \mathrm{sec}^{-1}$) after the onset of shear flow. Circles and solid line denote the data for the former and the latter, respectively.

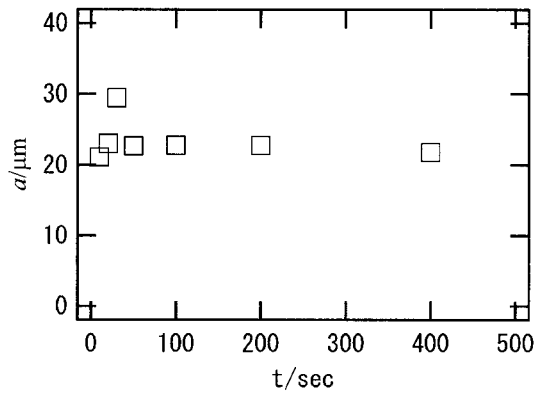

Fig. 7. Time dependence of number averaged shorter diameter a for the same sample as in Fig. 6.

Takahashi *et al.* (2000), such elongated domains burst to small droplets when the flow is stopped, therefore, shorter diameter a of the domains under the flow are examined for this sample. Fig. 7 shows time dependence of a. It is clear that there exists an overshoot in the time dependence of a, denoting existence of domains having larger size than expected for $\dot{\gamma}_f$.

In Fig. 6, the data for broad distribution sample ($\dot{\gamma}_{pre} = 0.8$, $\dot{\gamma}_f = 2.4\ \mathrm{sec}^{-1}$) is also shown for comparison. There exist a shallow undershoot due to the elongated domains. The undershoot of bimodal distribution sample is slightly larger than that for the broad distribution sample as can be seen in the inlet of Fig. 6. Since the number of large domains which break-up under the flow is greater for the broad distribution sample before onset of the flow, the undershoot should be smaller for the bimodal distribution sample. Therefore the observed larger undershoot implies

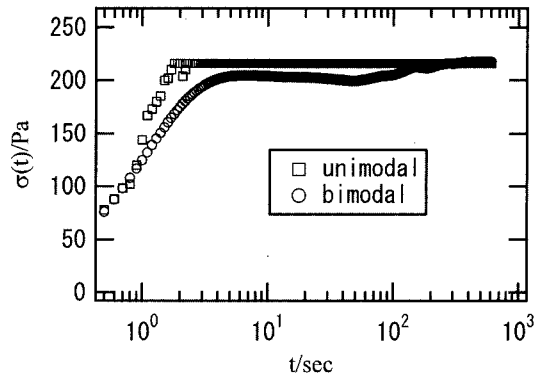

Fig. 8. Transient stress $\sigma(t)$ for a unimodal ($\dot{\gamma}_{pre} = 12.0\ \mathrm{sec}^{-1}$) and a bimodal distribution ($\dot{\gamma}_{pre1} = 7.2$, $\dot{\gamma}_{pre2} = 12.0\ \mathrm{sec}^{-1}$) samples after the onset of shear flow with $\dot{\gamma}_f = 7.2\ \mathrm{sec}^{-1}$.

the generation of larger domains and there elongation at the initial stage of flow. Thus, it is also concluded that the coalescence between large and small domains take place at the initial stage of the shear flow even in the bimodal distribution sample in which break-up of larger domains should occur.

The condition for the third bimodal distribution sample ($\dot{\gamma}_{pre1} = \dot{\gamma}_f$) corresponds to the most stable condition for the larger domains generated by $\dot{\gamma}_{pre1}$, since they already have steady state size at $\dot{\gamma}_f$. From above results, it is expected that larger domains will be also generated by the coalescence between large and small domains in the initial stage of coalescence process even in this case. Fig. 8 shows transient stress for the sample with $\dot{\gamma}_{pre1} = 7.2$, $\dot{\gamma}_{pre2} = 12.0$ and $\dot{\gamma}_f = 7.2\ \mathrm{sec}^{-1}$. It is clear that there exist an undershoot for the bimodal distribution sample denoting the generation of larger size domains and their elongation. From these results, we conclude that coalescence of large and small domains in the bimodal distribution samples at the initial stage of the coalescence process is a general characteristic. The generated large domains larger than those at the final steady states are then elongated and break-up to the smaller domains at the final steady states.

References

Doi, M. and T. Ohta, 1991, Dynamics and rheology of complex interfaces. I, *J. Chem. Phys.* **95**, 1242-1248.

Kitade, S., A. Ichikawa, N. Imura, Y. Takahashi and I. Noda, 1997, Rheological properties and domain structures of immiscible polymer blends under steady and oscillatory shear flows, *J. Rheol.* **41**, 1039-1060.

Nakatani, A.I. and M.D. Dadmun, 1995, Flow-induced structure in polymers, American Chemical Society, Washington DC.

Rusu, D. and E. Peuvrel-Disdier, 1999, In situ characterization by small angle light scattering of the shear-induced coalescence mechanisms in immiscible polymer blends, *J. Rheol.* **43**, 1391-1409.

Takahashi, Y., N. Kurashima, I. Noda and M. Doi, 1994a, Exper-

imental tests of the scaling relation for textured materials in mixtures of two immiscible fluids, *J. Rheol.* **38**, 699-712.

Takahashi, Y., S. Kitade, N. Kurashima and I. Noda, 1994b, Viscoelastic properties of immiscible polymer blends under steady and transient shear flows, *Polymer J.*, **26**, 1206-1212.

Takahashi, Y. and I. Noda, 1995, Domain structures and viscoelastic properties of immiscible polymer blends under shear flow, *ACS Symposium Series* **597**, 140-152.

Takahashi, Y., M. Suzuki and I. Noda, 2000, Examination of condition for fine structure of immiscible polymer blends by step change of shear rate, *Zairyo (J. Soc. Materials Sci., Japan)* **49**, 1286-1290.

Takahashi, Y. and Y. Akazawa, 2005, Hysteresis in domain size of imamiscible polymer blends under shear flow and the related viscosity behavior, *Nihon Reoloji Gakkaishi (J. Soc. Rheol. Japan)* **33**, 17-21.

Takahashi, Y. and T. Kato, 2005, Coalescence behavior of dispersed domains in imamiscible polymer blends having broad size distribution, *Nihon Reoloji Gakkaishi (J. Soc. Rheol. Japan)* **33**, 37-39.

Taylor, G.I., 1932, The viscosity of a fluid containing small drops of another fluid, *Proc. R. Soc. London.* Ser. A **138**, 41-48.

Taylor, G.I., 1934, The formation of emulsions in definable fields of flow, *Proc. R. Soc. London.* Ser. A **146**, 501-523.

Utracki, L.A., 1989, Polymer alloys and blends, Hanser, Munich.

Vinckier, I., P. Moldenaers and J. Mewis, 1996, Relashonship between rheology and morphology of model blends in steady shear flow, *J. Rheol.* **40**, 613-631.